A 60-GHz Horizontally Polarized Magneto-Electric Dipole Antenna Array with Two Dimensional Multi-Beam End-Fire Radiation

Jingxue Wang, Yujian Li, *Member*, *IEEE*, Lei Ge, *Member*, *IEEE*,
Junhong Wang, *Senior Member*, *IEEE* and Kwai-Man Luk, *Fellow*, *IEEE*

***Abstract*—A novel substrate integrated waveguide (SIW) fed horizontally polarized end-fire magneto-electric (ME) dipole antenna composed of an open-ended SIW with broad walls vertical to substrates and a pair of electric dipoles realized by four metallic patches is proposed. Simple configuration and excellent performance including an impedance bandwidth of 46.5%, stable gain of around 6 dBi and symmetrical cardioid radiation patterns with low backward radiation and low cross polarizations are achieved. An SIW 90° twist integrated in three-layered substrate is implemented in order to connect the ME-dipole antenna conveniently to the SIW beam-forming network with broad walls parallel to substrates. A 4 × 4 SIW Butler matrix with a three-layered zigzag topology is then designed, which enables a size reduction of 45% for the matrix compared with conventional single-layered configuration but not affecting its operating characteristics. By employing a 2 × 4 ME-dipole array with 90° twists, two folded Butler matrices and four SIW 3-dB E-plane couplers, a multi-beam end-fire array that can radiate eight beams scanning in two dimensions is designed at the 60-GHz band. The fabricated prototype verifies a wide impedance bandwidth of 22.1%, gain varying from 10 to 13 dBi and stable radiation beams can be obtained. Due to good performance and the compact structure with low fabrication costs, the proposed design would be attractive for future millimeter-wave wireless applications including 5G communications and the WiGig system.**

***Index Terms*—Substrate integrated waveguide (SIW), magneto-electric (ME) dipole antenna, multi-beam antenna array, end-fire, millimeter waves, 5G communications.**

I. Introduction

Multi-beam antenna arrays fed by passive beam-forming networks that have simple structure, low fabrication costs, low insertion loss and the ability to cover a wide area with a number of high directivity radiation beams have attracted increasing attention for applications at the millimeter-wave spectrum recently. Different types of transmission lines have been employed to build several millimeter-wave planar passive beam-forming networks. Butler matrixes consisting of microstrip lines and coplanar waveguides (CPWs) were reported in [1]-[5]. Single-layered configurations can be obtained but the insertion loss properties of these designs are degraded by the relatively large transmission loss of the microstrip line and CPW. Better transmission characteristics can be achieved by the waveguide structures at millimeter-wave frequencies. The substrate integrated waveguides (SIW) or the post-wall waveguides have been utilized for realizing the single-layered beam-forming networks of the multi-beam arrays with promising performance [6]-[9]. However, due to the relatively large width of the SIW, these beam-forming networks usually suffer from a bulky configuration. Moreover, a single-layered structure is difficult to provide enough degree of freedom in the design of the feed network for a two dimensional (2-D) multi-beam array.

As one of the possible applications in future millimeter-wave wireless communications, the multi-beam antenna arrays for portable devices, including the cellular phone and the tablet have been investigated in [10], [11]. It has been found that the arrays with multi-beam end-fire radiation, i.e. the radiation beams directing to the lateral edges of the devices, would be more promising because of its ability to save spacing occupied by antenna elements and also mitigate the undesirable influence of user's hand on the antenna radiation characteristics. Obviously, the radiating elements play a vital role in the achievable performance of the end-fire antenna array. End-fire antennas with high directivity, including the Yagi-Uda antenna [12], the horn antenna [13] and the dielectric rod antenna [14], are not suitable for the multi-beam array design due to their narrow beamwidth. A microstrip line fed angled-dipole antenna with a simple configuration was investigated in [15]. Wide impedance bandwidth can be obtained but the cross polarization of radiation is relatively high. Dual-polarized radiation can be realized by the patch antenna reported in [10]. However, the complex multi-layered geometry of the antenna makes it not easy to fabricate. In order to connect with the SIW beam-forming networks, end-fire antenna elements with SIW

Manuscript received by *, 2016. This work was supported in part by the National Natural Science Foundation of China under Grant No. 61671052, the National Nature Science Foundation of China under Grant No. 61331002 and a grant from the Research Grants Council of the Hong Kong SAR, China [Project No. 9042377 (CityU 11277116)].

J. X. Wang, Y. J. Li and J. H. Wang are with the Institute of Lightwave Technology, Beijing Jiaotong University, Beijing 100044, China (Corresponding author e-mail: liyujian@bjtu.edu.cn).

L. Ge is with the College of Electronic Science and Technology, Shenzhen University, Shenzhen, China. (e-mail: leige@szu.edu.cn).

K. M. Luk is with the State Key Laboratory of Millimeter Waves, and Department of Electronic Engineering, City University of Hong Kong, Hong Kong, China

This article has been accepted for publication in a future issue of this journal, but has not been fully edited. Content may change prior to final publication. Citation information: DOI 10.1109/TAP.2017.2754328, IEEE Transactions on Antennas and Propagation

feed have also been studied. The end-fire post-wall waveguide-aperture antenna with an impedance bandwidth of 11% and unsymmetrical radiation pattern was reported in [16]. More recently, by applying the concept of the magneto-electric (ME) dipole that was originally introduced in [17], a wideband antenna element with end-fire radiation has also been realized in [11]. However, all these designs are vertically polarized due to the constraint of the electric field direction of TE_{10} mode propagating along the feeding SIW.

For the purpose of enriching the polarization manners of the SIW fed end-fire antennas, which is important for further enhancing the channel capacity of millimeter-wave wireless communications by the use of polarization diversity, a novel horizontally polarized end-fire ME-dipole antenna is proposed in the 60-GHz band in this paper. The combination of a three-layered open-ended SIW with the electric field lying along horizontal direction and four metal patches enables the radiating element with wide impedance bandwidth, symmetrical radiation pattern with low cross polarization, low backward radiation and stable gain. Additionally, with the help of a new SIW 90° twist integrated into three substrates, the proposed ME-dipole antenna with horizontal polarization can still be excited by the conventional SIW conveniently. After that, in order to decrease the dimension of the passive beam-forming network, a folded 4 × 4 SIW Butler matrix with a zigzag topology is implemented in three-layered substrates. The compact configuration can be achieved but not affecting the operating performance of the design. By employing the horizontally polarized ME-dipole antennas and the folded beam-forming networks, a 2 × 4 antenna array that can generate eight end-fire radiation beams scanning in two dimensions is designed, fabricated and measured. Good characteristics are demonstrated by the fabricated prototype.

The paper is organized as follows. The detailed geometry and working mechanism of the proposed horizontally polarized end-fire ME-dipole antenna as well as the SIW 90° twist are described in Section II. Section III presents the geometry and simulated results of the three-layered folded Butler matrix. Design considerations of the multi-beam antenna array are depicted in Section IV and the measured results are discussed in Section V. A brief conclusion is finally given in Section VI.

II. Magneto-Electric Dipole Antenna

A. Horizontally Polarized Magneto-Electric Dipole

As aforementioned, the SIWs with broad walls parallel to horizontal substrates are usually applied to feed the end-fire antennas, which leads to the vertical polarization of these designs. Another kind of laminated waveguide structure with broad walls vertical to the integrating substrates was also reported in [18], but it was seldom used for antenna design. In this paper, this concept is realized in three stacked PCB substrates. By employing this structure as the feeding scheme, a novel SIW-fed ME-dipole antenna with horizontally polarized end-fire radiation can be implemented successfully.

The geometry of the proposed ME-dipole antenna is presented in Fig. 1, where the whole structure is integrated into

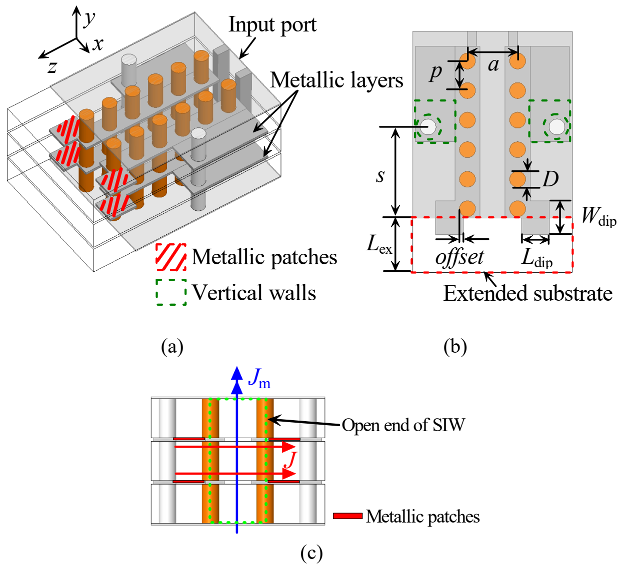

Fig. 1. Geometry of the proposed horizontally polarized end-fire ME-dipole antenna. (a) Perspective view, (b) Top view. (c) Front view.

three printed circuit board (PCB) laminates. The two columns of metallic vias indicated in orange in Fig. 1 and the metallic layers are combined together to compose two metallic lattice arrays in vertical direction, i.e. *y*-axis, which work as the broad walls of the SIW. On the other hand, the top and the bottom metallic layers in Fig. 1 (a) are used as the side walls of the SIW. Therefore, the antenna can be excited by the TE_{10} mode within the SIW with the electric field lying along horizontal direction.

As discussed in [17], a combination of an electric dipole and a magnetic dipole orthogonal to each other is required in order to realize the ME-dipole antenna. In this design, the radiating aperture of the open-ended SIW can be seen as an equivalent magnetic dipole J_m radiating in vertical direction according to the equivalence principle. Two pairs of metallic patches operating as two electric dipoles J in horizontal direction are introduced into the middle two metallic layers as shown in Fig. 1. Since the four patches are connected to the broad walls of the open-ended SIW, a portion of the radiation power is coupled to the patches and thus the electric dipoles can be excited effectively. In order to tune the input impedance of the antenna, the substrates in front of the radiating aperture are extended toward the direction of *z*-axis. Furthermore, two columns of metallic pins characterized in white are added into the design as depicted in Fig. 1. The pins are combined with the metallic layers to realize two lattice arrays behind the antenna. Since the size of the metallic lattices is small in comparison with the operating wavelength, they can be approximately seen as two metallic walls in this design. For the antenna array that will be discussed in Section IV, the vertical walls can effectively isolate the radiating elements with other devices located behind the array. In this design, all substrates are Rogers 5880 PCB laminates with a thickness of 0.787 mm and a dielectric constant of 2.2. The antenna is designed with the help of a full-wave electromagnetic solver Ansys HFSS [19].

The design guideline of this antenna is similar to those given in [16]. By properly adjusting the dimensions of the metallic

This article has been accepted for publication in a future issue of this journal, but has not been fully edited. Content may change prior to final publication. Citation information: DOI 10.1109/TAP.2017.2754328, IEEE Transactions on Antennas and Propagation

TABLE I
DIMENSIONS OF THE ME-DIPOLE ANTENNA (UNITS: mm)

Parameters	***p***	***D***	***a***	L_{ex}
Values	0.65	0.35	1.1	1.3
Parameters	***s***	***offset***	L_{dip}	W_{dip}
Values	2.2	-0.09	0.45	0.75

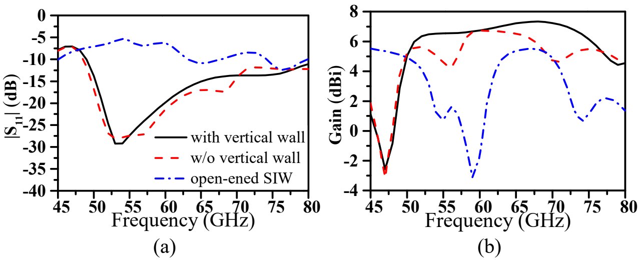

Fig. 2. Simulated results of the proposed horizontally polarized ME-dipole antenna. (a) $|S_{11}|$ and (b) Gain.

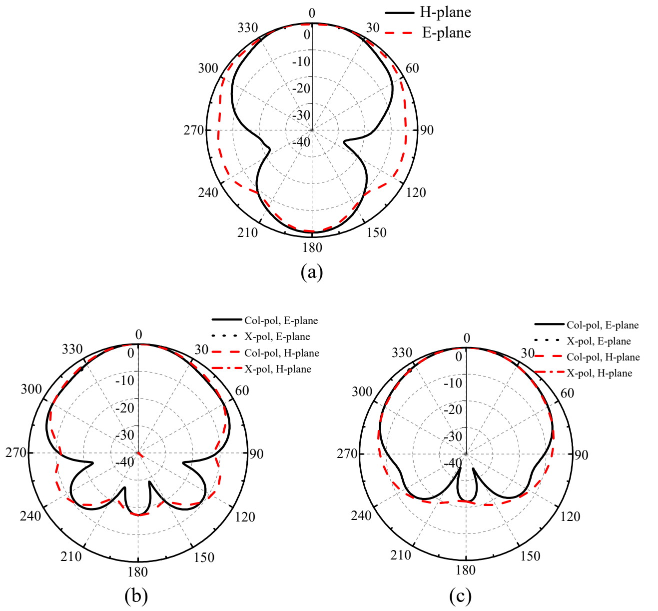

Fig. 3. Simulated radiation patterns of the three antennas at 60 GHz. (a) Open-ended SIW, (b) ME-dipole antenna without vertical walls, (c) ME-dipole antenna with vertical walls.

patches W_{dip} and L_{dip}, the distance between the edge of the metallic patches and the vias of the SIW *offset*, and the length of the extended substrates L_{ex}, the electric dipoles in horizontal direction and the equivalent magnetic dipole in vertical direction in this design can be excited in phase with similar magnitudes. Hence, a ME-dipole antenna with horizontally polarized radiation in the end-fire direction can be obtained. The final values of the parameters of the proposed design are listed in Table I.

The simulated $|S_{11}|$ and gain of the open-ended SIW and the ME-dipole antennas with and without the vertical walls are shown in Fig. 2. It should be noted that the open-ended SIW antenna employed here for comparison refers only to the open-ended SIW shown in Fig. 1, which radiates as a magnetic dipole J_m with horizontal polarization. It is seen in Fig. 2 that the open-ended SIW structure without the metallic patches suffers from a poor impedance matching and an unstable gain performance. By adding the two electric dipoles, an impedance bandwidth of 46.5% for $|S_{11}| < -10$ dB (from 49 to 78.7 GHz) and stable gain up to 7.3 dBi with a variation of less than 2.3 dB across the operating band can be achieved. Additionally, the simulated results of the designs with and without the vertical walls are similar to each other. It means that the added walls do not affect the performance of the design significantly.

The simulated radiation patterns of the three designs are illustrated in Fig. 3. The typical radiation pattern of a magnetic dipole can be observed in Fig. 3 (a), which validates the working mechanism of the open-ended SIW. As shown in Fig. 3 (b) and (c), there is no remarkable effect on the radiation pattern caused by the existence of the vertical wall. The radiation patterns of the proposed horizontally polarized ME-dipole antenna are almost identical in the E- and H- planes. The 3-dB beamwidth of the radiation pattern is around 80°. The backward radiation and the cross polarization level are less than – 20 dB and -40 dB, respectively.

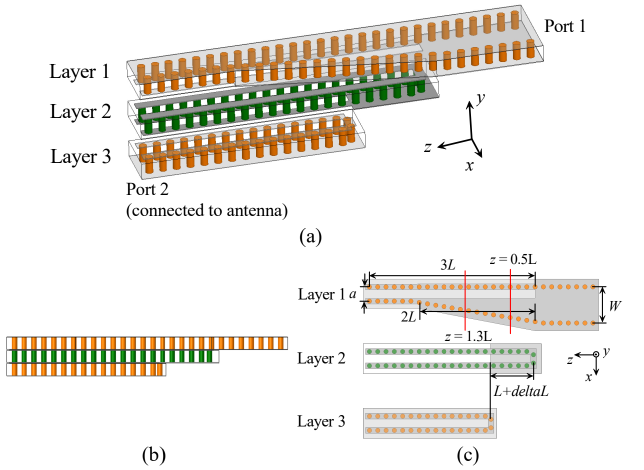

Fig. 4. Geometry of the proposed SIW 90° twist. (a) Perspective view, (b) Side view, (c) Top views of the three substrates.

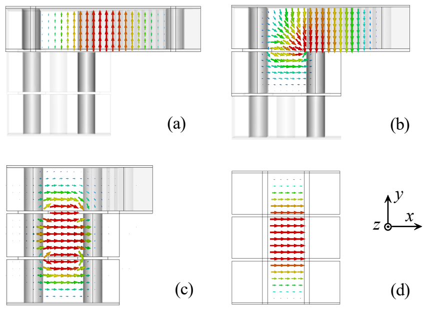

Fig. 5. Electric field distributions at different positions within the SIW 90° twist. (a) Port 1, (b) $z = 0.5L$, (c) $z = 1.3L$, (d) Port 2.

B. Substrate Integrated Waveguide 90° Twist

For convenience of connecting the proposed horizontally polarized ME-dipole antenna designed in the above section with the beam-forming network composed of SIWs with broad walls parallel to substrates, a SIW 90° twist should be inserted

This article has been accepted for publication in a future issue of this journal, but has not been fully edited. Content may change prior to final publication. Citation information: DOI 10.1109/TAP.2017.2754328, IEEE Transactions on Antennas and Propagation

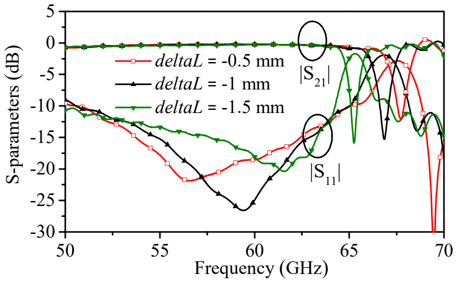

Fig. 6. Simulated S-parameters of the SIW 90° twist with different values of *deltaL*.

between the antenna and the feed network. By applying the LEGO-type structure, i.e. a stacking structure, a SIW 90° twist with three-dimensional configuration was realized in [20]. Nevertheless, as the design cannot be integrated into multi-layered planar substrates, it is not desirable for millimeter-wave antenna realization. In order to resolve the issue, a new SIW 90° twist with a three-layered form is designed in this section as illustrated in Fig. 4, where Port 1 connecting to the feed network is located at the top substrate Layer 3, and Port 2 used for exciting the antenna with horizontal polarization is arranged in the three layers. It is seen that the width of the SIW along the horizontal direction gradually decreases from W to a within a length of $2L$ in Layer 3, while a slit is etched in the bottom metallic surface of Layer 3 at the same time. On the other hand, with the location moving forward along the z-axis, another two slits are cut in the bottom metallic surfaces of Layers 2 and 1 respectively. As a result, the height of the SIW in the vertical direction increases with a step of the thickness of the substrate when the width of the SIW in the horizontal direction reduces. Moreover, the total width of the SIW structure can be kept constant throughout the 90° twist. Fig. 5 depicts the electric field distributions at four different positions in the z-axis that are marked by red lines in Fig. 4 (b). It can be revealed clearly that the electric field direction of the TE_{10} mode propagating in the SIW is rotated effectively from the vertical polarization at Port 1 to the horizontal polarization at Port 2.

It is found that the value of *deltaL* has a crucial impact on the operating band of the proposed SIW 90° twist as shown in Fig. 6. Based on the parametric studies, the final value of *deltaL* is set to -1 mm, while the parameters L and W are determined to 4 and 2.83 mm respectively. The simulated operating bandwidth of the twist is 25.1% for $|S_{11}| < -10$ dB (from 50.5 to 65 GHz). As a conclusion, the 3-layered SIW90° twist provides an effective mean to connect the horizontally polarized ME-dipole array with the beam-forming network that will be discussed in the following section.

III. Folded 4 × 4 Butler Matrix

The SIW Butler matrix is a promising choice for realizing a passive millimeter-wave multi-beam antenna array. However, its relatively large dimension would increase the whole size of the array, which is not desirable for the design of compact millimeter-wave wireless systems. The geometry of a traditional single-layered 4 × 4 SIW Butler matrix operating in

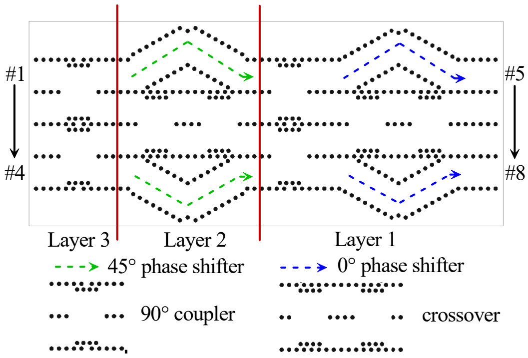

Fig. 7. Geometry of the traditional single-layered 4 × 4 SIW Butler matrix.

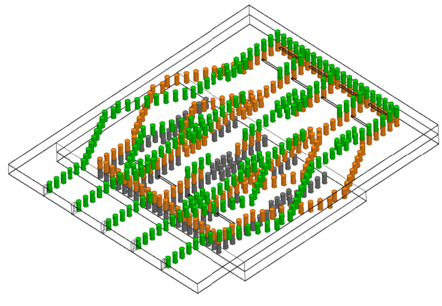

(a)

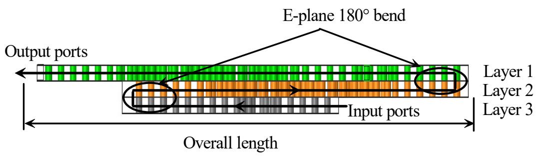

(b)

Fig. 8. Side view of the proposed 3-layered 4 × 4 Butler matrix. (a) Perspective view, (b) Side view.

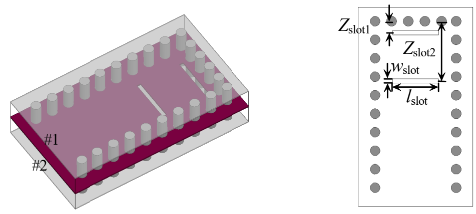

(a) (b)

Fig. 9. Geometry of the SIW E-plane 180° bend. (a) Perspective view, (b) Top view with dimensions.

the 60-GHz band is shown in Fig. 7, where the overall length of the design is 41.4 mm. In order to reduce the size, the matrix is divided into three portions in the manner of the red lines indicated in Fig. 7. Then these parts are arranged into three stacked substrates with a zigzag-shaped topology as depicted in Fig. 8. The input and output ports of the feed network are located in the bottom substrate Layer 3 and the top substrate Layer 1, respectively. By this mean, the entire length of the four-way SIW Butler matrix can be decreased to 22.9 mm, which means that a size reduction of 45% can be achieved compared with the original geometry.

As shown in Fig. 8, two sets of E-plane 180° bend structures are required for the modified Butler matrix design. The detailed geometry of the bend is exhibited in Fig. 9. Two short-ended SIW sections are designed at the same location of two adjacent substrates. Two transverse slots with same dimensions are

This article has been accepted for publication in a future issue of this journal, but has not been fully edited. Content may change prior to final publication. Citation information: DOI 10.1109/TAP.2017.2754328, IEEE Transactions on Antennas and Propagation

Table II
DIMENSIONS OF THE E-PLANE 180° BEND (UNITS: mm)

Parameters	Z_{slot1}	Z_{slot2}	l_{slot}	w_{slot}
Values	0.4	2.1	1.6	0.15

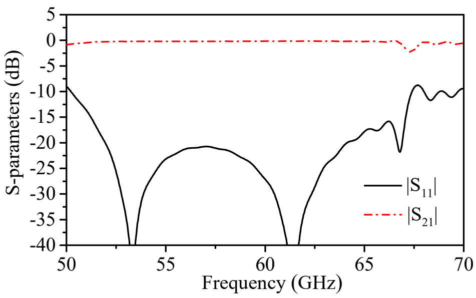

Fig. 10. Simulated S-parameters of the E-plane 180° bend.

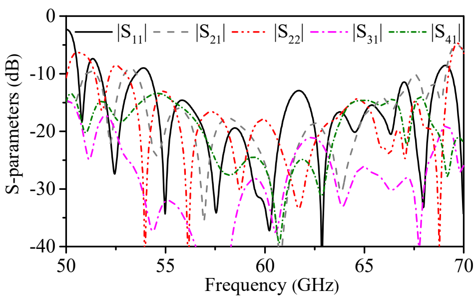

Fig. 11. Simulated S-parameters of the proposed 3-layered 4 × 4 Butler matrix.

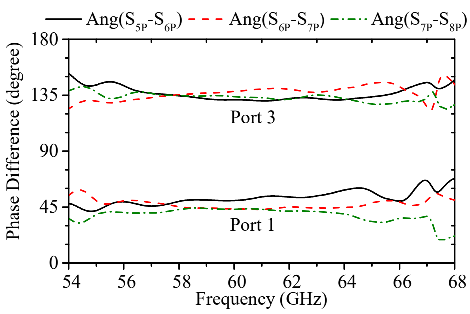

Fig. 12. Simulated phase response of the proposed 3-layered 4 × 4 Butler matrix.

etched in the common broad wall of the two SIW sections for power coupling between the two layers. Final values of the dimensions of the 180° bend are concluded in Table II and Fig. 10 gives the simulated performance. It can be seen that the operating bandwidth is 29.3% for $|S_{11}| < -10$ dB (from 50.2 to 67.4 GHz).

The simulated S-parameters and phase responses of the proposed 3-layered Butler matrix are shown in Fig. 11 and Fig. 12, respectively. Reflection coefficients of less than -10 dB and the phase error of less than ±15° can be achieved over a wide bandwidth of 23.6% (from 54.2 to 68.7 GHz), which verifies that a notable size reduction can be realized successfully by the proposed SIW Butler-matrix but not degrading its performance.

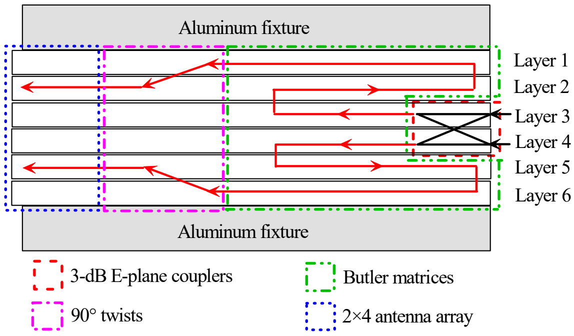

Fig. 13. Side view of the proposed 2 × 4 multi-beam end-fire array.

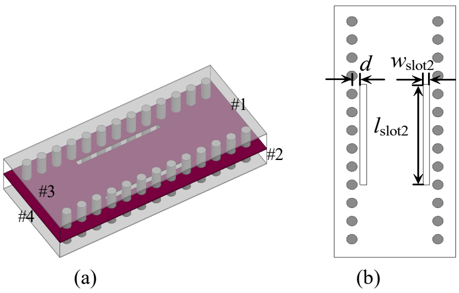

Fig. 14. Geometry of the E-plane 3-dB coupler. (a) Perspective view, (b) Top view with dimensions.

Table III
DIMENSIONS OF THE E-PLANE 3-dB COUPLER (UNITS: mm)

Parameters	w_{slot2}	l_{slot2}	d
Values	0.22	3.6	0.27

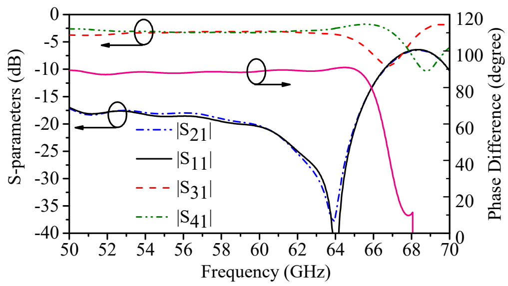

Fig. 15. Simulated S-parameters and phase response of the 3-dB E-plane SIW coupler.

It should be noted that the detailed dimensions not given are same with those of the design in [11].

IV. TWO-DIMENSIONAL EIGHT-BEAM END-FIRE ARRAY

By employing the horizontally polarized ME-dipole antennas and the folded SIW Butler matrixes discussed above, a 2 × 4 antenna array that can generate eight end-fire radiation beams scanning in two dimensions is implemented in this section. The side view of the array configuration is illustrated in Fig. 13. Two three-layered 4 × 4 Butler matrixes are integrated into substrate Layers 1 to 3 and Layers 4 to 6, respectively. The output ports of the two matrices are linked to the 2 × 4 antenna array with 90° SIW twists. The eight input ports of the two matrixes that are located in neighboring Layers 3 and 4 are

This article has been accepted for publication in a future issue of this journal, but has not been fully edited. Content may change prior to final publication. Citation information: DOI 10.1109/TAP.2017.2754328, IEEE Transactions on Antennas and Propagation

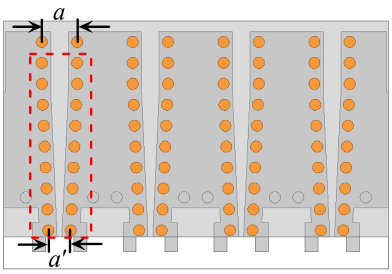

Fig. 16. Top view of the geometry of the 1 × 4 antenna array with tapered structures.

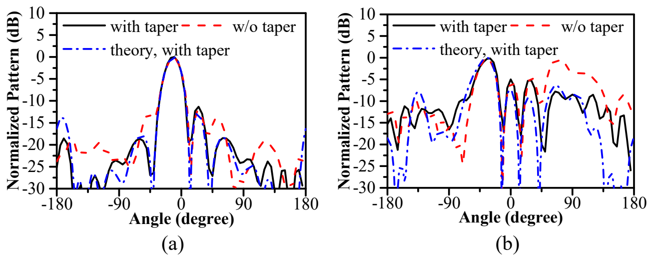

Fig. 17. Radiation patterns of the 1 × 4 antenna array with and without the taper. (a) 45°phase difference between the input ports, (b) 135° phase difference between the input ports.

connected separately by applying four SIW E-plane 3-dB couplers. Therefore, the power from the input ports of the array can go through the beam-forming network as indicated in Fig. 13 and finally excite the antenna array. Compared with the SIW beam-forming network with the single-layered topology that can realize the same function, at least 77.5% of spacing in horizontal plane can be saved by the proposed design. More importantly, by introducing the degree of freedom in vertical direction, different portions of the antenna array can be connected directly without the use of delay lines or crossovers, which can reduce the length of the paths throughout the beam-forming network and thus decreases the undesired insertion loss. As shown in Fig. 13, the six stacked PCB laminates consisting of the antenna array is assembled by two aluminum fixtures. The geometry of the SIW E-plane 3-dB coupler is illustrated in Fig. 14, where the two longitudinal slots are cut on the common broad wall of the two SIWs. Values of the dimensions are collected in Table III. The simulated operating bandwidth of the coupler is 27% for $|S_{11}| < -15$ dB (from 50 to 65.6 GHz) as presented in Fig. 15. Besides, the phase error is less than 5° over this band.

The element spacing of the 1 × 4 ME-dipole array shown in Fig. 16 is 2.83 mm (0.57 λ_0 at 60 GHz), which is equal to the width of the SIW used for composing the beam-forming network. It is found in the design procedure that the small element spacing would result in the unacceptable sidelobe level of the radiation pattern as shown in Fig. 17. In order to overcome the issue, a tapered configuration in the red frame in Fig. 16 is adopted by the antenna elements. In this region, the height of the feeding SIW a is tapered from 1.1 mm to 0.7 mm. The dimensions of the electric dipoles should be adjusted slightly as well to get better impedance matching. With the help of this modification, the mutual coupling characteristics and the radiation pattern of the array can be improved effectively. The

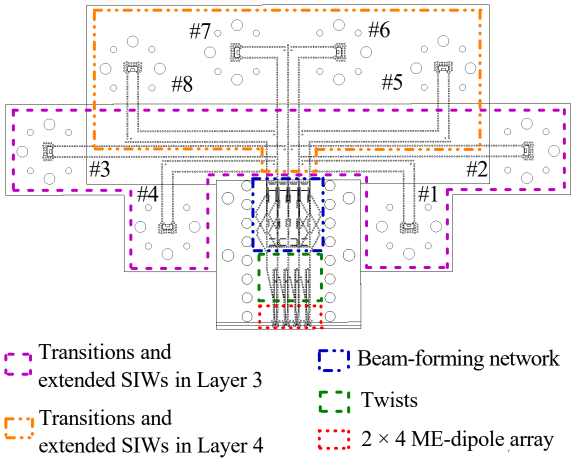

Fig. 18. Top view of the geometry of the antenna array with SIW to air-filled waveguide transitions.

simulated radiation patterns of the 1 × 4 ME-dipole array with the tapered structures and the theoretical results calculated from the produce of the radiation pattern of a single element and the array factor are also given in Fig. 17, which verifies the effectiveness of this modification. However, it can be observed that the first sidelobe level of the beam directing to around 45° is still relatively high. This is mainly because the element spacing of greater than 0.5 λ_0 at 60 GHz. Better sidelobe level can be achieved by employing smaller element spacing of the array.

Based on the above considerations, the top view of the entire configuration of the multi-beam array is shown in Fig. 18. For the sake of measurement, the input ports of the array are extended outward and connected to eight wideband SIW to air-filled waveguide transitions developed previously in [21].

V. Measurement and Discussion

A prototype of the designed multi-beam antenna array with horizontally polarized end-fire radiation beams was implemented by standard PCB facilities as presented in Fig. 19. During the measurement, the ports that were not under test were connected with WR-15 waveguide loads. The S-parameters of the array were performed by a millimeter-wave band Agilent Network Analyzer E8361A with two ports. The radiation performance was measured by adopting an *NSI* 2000 near-field measurement system. The gain of the array was obtained by comparison with a standard horn.

A. Impedance Bandwidth and Isolation

Measured and simulated S-parameters are given in Fig. 20 with good agreement. The measured and simulated overlapped bandwidths of the array for S-parameters of less than -10 dB are 22.1% (from 52.3 to 65.3 GHz) and 25.3 % (from 51.8 to 66.8 GHz) respectively. A slight shift of around 0.8 GHz in frequency between the measured and simulated results would mainly result from the fabrication tolerance. The results of $|S_{55}|$ to $|S_{88}|$ should be similar to those of ports 1 to 4 due to the symmetry of the array configuration. The measured results above 67 GHz are not available because of the frequency limit of the used network analyzer.

This article has been accepted for publication in a future issue of this journal, but has not been fully edited. Content may change prior to final publication. Citation information: DOI 10.1109/TAP.2017.2754328, IEEE Transactions on Antennas and Propagation

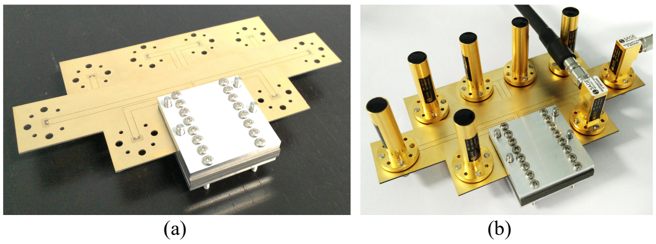

Fig. 19. Fabricated prototype of the proposed 2 × 4 horizontally polarized multi-beam end-fire antenna array. (a) Top view, (b) Back view.

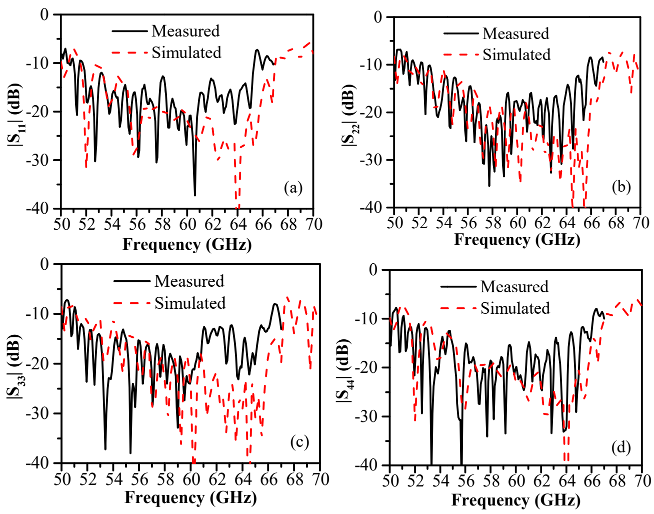

Fig. 20. Measured and simulated S-parameters of the proposed antenna array.

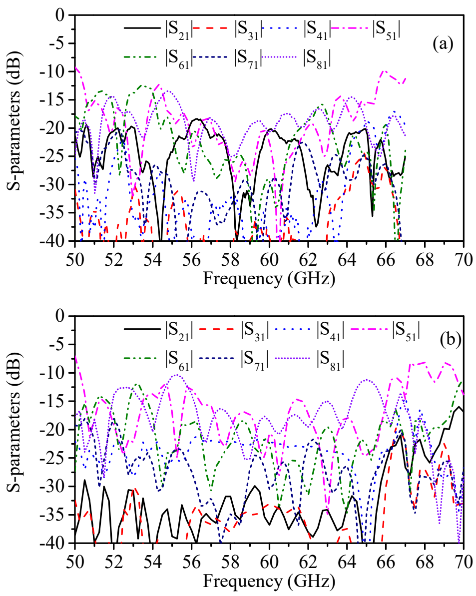

Fig. 21. Measured and simulated isolations of the proposed antenna array. (a) Measured, (b) Simulated.

The measured isolations between port 1 and ports 2 to 8 illustrated in Fig. 21 (a) also agree well with the simulated results in Fig. 21 (b). The measured isolations are almost larger than 15 dB within the operating band from 55 to 66 GHz.

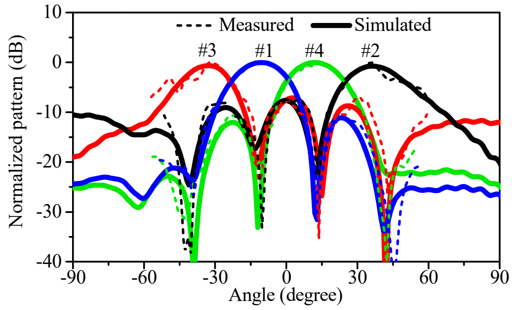

Fig. 22. Measured and simulated E-plane radiation patterns of the proposed antenna array at 60 GHz.

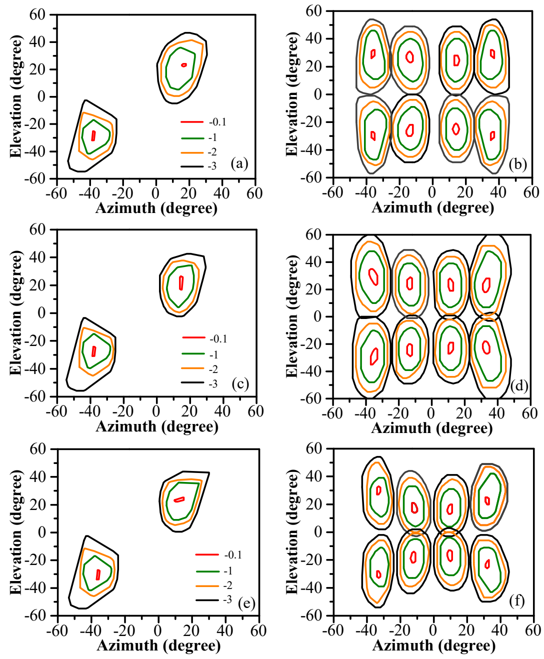

Fig. 23. The contour of the measured and simulated 3-dB radiation beams generated by the proposed multi-beam antenna array. (a) Measured at $f = 55$ GHz, (b) Simulated at $f = 55$ GHz, (c) Measured at $f = 60$ GHz, (d) Simulated at $f = 60$ GHz, (e) Measured at $f = 65$ GHz, (f) Simulated at $f = 65$ GHz.

B. Radiation Pattern

Measured and simulated E-plane radiation patterns at 60 GHz when the four ports of the same Butler matrix are excited respectively are given in Fig. 22. The four beams scanning in the horizontal plane can cover an angular range of around 70°. Furthermore, the sidelobe is almost less than -10 dB. The contours of the eight 3-dB radiation beams generated by the antenna array are presented in Fig. 23, where satisfying agreement between measured and simulated results can be seen. The radiation beams are stable over the operating band from 55 to 65 GHz. The measured radiation beams when other ports are excited should be similar to the results shown in Fig. 23 due to the symmetry of the array configuration.

C. Gain and Efficiency

Measured and simulated gain and directivity of the antenna array when ports 1 and 2 are excited separately are shown in Fig. 24 with good agreement. The measured gain for feeding from Port 1 is up to 13.1 dBi with a variation of 2 dB within the operating band from 55 to 65 GHz, while the counterpart for

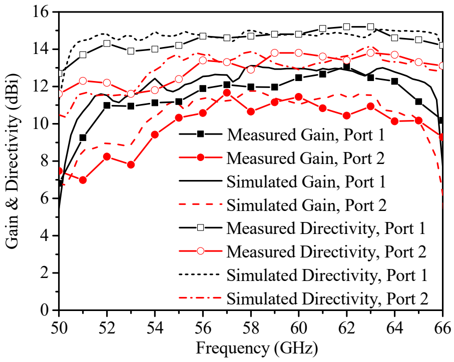

Fig. 24. Measured and simulated gain and directivity of the proposed antenna array.

feeding from Port 2 is up to 11.7 dBi with a variation of 1.8 dB throughout the same band. The directivities of the antenna array are around 14.5 dBi and 13 dBi respectively for excitation from Port 1 and Port 2. Hence, the measured radiation efficiency of the array should be approximately 60% by comparing the results of gain and directivity. According to the results presented in Sections II to IV, the simulated insertion losses of the Butler matrix, 3-dB coupler, 90° twist and antenna element are 1.2, 0.1, 0.4 and 0.35 dB, respectively. Therefore, the loss of entire antenna array should be around 2.05 dB. The radiation efficiency calculated from the result is 62%, which is close to the measured one. The slight difference between the measured and simulated results would be due to the uncertainty of dielectric loss of the substrates in V-band, and the possible fabrication and alignment tolerances. It should be noted that the insertion losses from the extending SIW sections and the waveguide to SIW transitions have been calibrated.

D. *Comparison and Discussion*

The configuration features and operating characteristics of the proposed and reported millimeter-wave multi-beam antenna arrays with passive beam-forming networks are summarized in Table IV for comparison. Most reported 2-D multi-beam arrays can only generate the beams scanning in planes vertical to the antenna array. In this design, by applying the proposed multi-layered SIW beam-forming network with compact configuration, 2-D multi-beam radiation can be realized in the end-fire plane. Moreover, thanks to the low-loss properties of the SIW beam-forming network, better gain performance can be achieved by this work in comparison with the designs in [2] and [21]. Besides, the operating bandwidth of the proposed array is also comparable with the reported wideband designs. The end-fire ME-dipole antenna investigated previously in [11] with vertical polarization and the ME-dipole antenna proposed in this paper pave the way for designing wideband multi-beam array with dual-polarized end-fire radiations.

VI. Conclusion

A magneto-electric dipole antenna with horizontally polarized end-fire radiation, a wide bandwidth of 46.5% and stable gain of around 6 dBi has been proposed. A substrate integrated waveguide 90° twist with simple three-layered configuration has also been accomplished to feed the antenna

Table IV
Comparison between Proposed and Reported Millimeter-Wave Passive Multi-Beam Antenna Arrays

Ref.	Antenna array	Radiation	Feed Network	BW	Gain (dBi)
[2]	2 × 4 (Patch)	2-D (Broadside)	MSL	12%	12.3
[9]	2 × 2 (Patch)	2-D (Broadside)	SIW	7.6%	12
[21]	2 × 2 (ME-dipole)	2-D (Broadside)	SIW	22%	12.5
[5]	1 × 8 (Angled Dipole)	1-D (End-fire)	MSL	18.2%	5.8
[11]	1 × 8 (ME-dipole)	1-D (End-fire)	SIW	16.4%	12
This work	2 × 4 (ME dipole)	2-D (End-fire)	SIW	22%	13.1

element. A compact beam-forming network consisting of two three-layered Butler matrixes with zigzag topology and four E-plane 3-dB couplers was implemented in six stacked substrates. With the combination of the proposed antenna elements and beam-forming network, a 2 × 4 magneto-electric dipole array that can generate eight horizontally polarized end-fire radiation beams scanning in two dimensions has been designed, fabricated and measured. An overlapped impedance bandwidth of 22.1%, stable radiation beams, and gain up to 13.1 dBi were achieved. The proposed magneto-electric dipole in this paper enriches the polarization properties of the millimeter-wave antenna with end-fire radiation fed by the substrate integrated waveguide. The design process of the substrate integrated multi-layered beam-forming network provides a mean to effectively decrease the dimensions of the millimeter-wave passive multi-beam antenna arrays. With compact structure, low costs and good performance, the proposed multi-beam array design would be a desirable candidate to future millimeter-wave wireless applications, such as 5G communications and the WiGig systems.

Acknowledgment

The authors are grateful to Dr. Wenhua Chen, Dr. K. B. Ng, Dr. Zilong Ma, Huan Yi, and Kaixu Wang for helping with the antenna measurement.

References

[1] C. Dall'omo, T. Monediere, B. Jecko, F. Lamour, I. Wolk, and M. Elkael, "Design and realization of a 4 × 4 microstrip butler matrix without any crossing in millimeter waves," *Microw. Opt. Technol. Lett.*, vol. 38, no. 6, pp. 462–465, Jul. 2003.

[2] William F. Moulder, Waleed Khalil, and John L. Volakis, "60-GHz Two-Dimensionally Scanning Array Employing Wideband Planar Switched Beam Network," *IEEE Antennas and Wireless Propagation Letters*, vol. 9, pp. 818–821, Aug. 2010.

[3] C. Tseng, C. Chen, and T. Chu, "A low-cost 60-GHz switched-beam patch antenna array with butler matrix network," *IEEE Antennas Wire-less Propag. Lett.*, vol. 7, pp. 432–435, 2008.

[4] M. Nedil and T. A. Denidni, "Novel butler matrix using CPW multilayer technology," *IEEE Trans. Microw. Theory Techn.*, vol. 54, no. 1, pp. 499–507 Jan. 2006.

[5] B. Cetinoneri, Y. A. Atesal, and G. M. Rebeiz, "An 8 × 8 Butler matrix in 0.13 m CMOS for 5–6-GHz multibeam applications," *IEEE Trans. Microw. Theory Tech.*, vol. 59, no. 2, pp. 295–301, Feb. 2011

This article has been accepted for publication in a future issue of this journal, but has not been fully edited. Content may change prior to final publication. Citation information: DOI 10.1109/TAP.2017.2754328, IEEE Transactions on Antennas and Propagation

[6] S. Yamamoto, J. Hirokawa, and M. Ando, "A beam switching slot array with a 4-way Butler matrix installed in a single layer post-wall waveguide", *IEEE Int Symp Antennas Propag*., pp. 138–141, Jun. 2002.

[7] T. Djerafi and K. Wu, "A low-cost wideband 77-GHz planar butler matrix in SIW technology," *IEEE Trans. Antennas Propag.*, vol. 60, no. 10, pp. 4949–4954, Oct. 2012.

[8] C.-J. Chen and T.-H. Chu, "Design of a 60-GHz substrate integrated waveguide butler matrix—A systematic approach," *IEEE Trans. Microw. Theory Techn.*, vol. 58, no. 7, pp. 1724–1733, Jul. 2010.

[9] A. B. Guntupalli, T. Djerafi, and K. Wu, "Two-dimensional scanning antenna array driven by integrated waveguide phase shifter," *IEEE Trans. Antennas Propag.*, vol. 62, no. 3, pp. 1117–1124, Mar. 2014.

[10] W. Hong, K.-H. Baek, Y. Lee, Y. Kim and S.-T. Ko, "Study and prototyping of practically large-scale mmWave antenna systems for 5G cellular devices," *IEEE Commun. Mag*., vol. 52, no. 9, pp. 63–69, Sep. 2014.

[11] Yujian Li and Kwai-Man Luk, "A multibeam end-fire magnetoelectric dipole antenna array for millimeter-wave applications," *IEEE Trans. Antennas Propag.*, vol. 64, no. 7, pp. 2894–2904, Jul. 2016.

[12] Ramadan A. Alhalabi and Gabriel M. Rebeiz, "High-gain Yagi-Uda antennas for millimeter-wave switched-beam systems," *IEEE Trans. Antennas Propag.*, vol. 57, no. 11, pp. 3672–3676, Nov. 2009.

[13] A. R. Mallahzadeh and S. Esfandiarpour, "Wideband H-plane horn antenna based on ridge substrate integrated waveguide (RSIW)," *IEEE Antennas Wireless Propag. Lett.*, vol. 11, pp. 85–88, 2012.

[14] N. Ghassemi and K. Wu, "Planar dielectric rod antenna for gigabyte chip-to-chip communication," *IEEE Trans. Antennas Propag.*, vol. 60, no. 10, pp. 4924–4928, Oct. 2012.

[15] R. A. Alhalabi and G. M. Rebeiz, "High-efficiency angled dipole antennas for millimeter-wave phased array applications," *IEEE Trans. Antennas Propag.*, vol. 56, no. 10, pp. 3136–3142, Oct. 2008.

[16] R. Suga, H. Nakano, Y. Hirachi, J. Hirokawa, and M. Ando, "Costeffective 60-GHz antenna package with end-fire radiation for wireless file-transfer system," *IEEE Trans. Microw. Theory Techn.*, vol. 58, no. 12, pp. 3989–3995, Dec. 2010.

[17] K.-M. Luk and H. Wong, "A new wideband unidirectional antenna element," *Int. J. Microw. Opt. Technol.*, vol. 1, no. 1, pp. 35–44, Jun. 2006.

[18] H. Uchimura, T. Takenoshita and M. Fujii, "Development of a 'laminated waveguide'," *IEEE Trans. Microw. Theory Techn.*, vol. 46, no. 12, pp. 2438-2443, Dec. 1998.

[19] Ansoft Corp., Canonsburg, PA, USA. *HFSS: High Frequency Structure Simulator Based on the Finite Element Method*. [Online]. Available: http://www.ansoft.com/

[20] A. Doghri, T. Djerafi, A. Ghiotto, and K. Wu, "SIW 90-degree twist for substrate integrated circuits and systems," in *IEEEMTT-S Int. Microw. Symp. Dig.*, Seattle, WA, USA, Jun. 2013, pp. 1–3.

[21] Yujian Li and Kwai-Man Luk, "60-GHz dual-polarized two-dimensional switch-beam wideband antenna array of aperture-coupled magneto-electric dipoles," *IEEE Trans. Antennas Propag.*, vol. 64, no. 2, pp. 554–563, Feb. 2016.

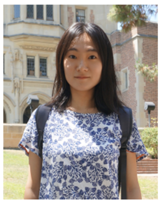

Jingxue Wang was born in Jilin, China. She received the B.Eng degree in electrical engineering from Beijing Jiaotong University, Beijing, China, in 2015 and is currently working towards the Ph.D. degree in electrical engineering at the same university.

Her research interests focus on millimeter wave antennas and arrays.

Miss Wang received the Best Student Paper Awards at UCMMT 2016 and ACES 2017.

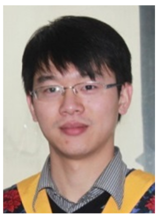

Yujian Li (S'12–M'15) was born in Hunan, China, in 1987. He received the B.S. and M.S. degrees in communications engineering from Beijing Jiaotong University, Beijing, China, in 2009 and 2012, respectively, and the Ph.D. degree in electronic engineering from City University of Hong Kong in 2015.

He joined the Institute of Lightwave Technology at Beijing Jiaotong University in 2015 as an Associate Professor. His current research interests include millimeter wave antennas, base station antennas and leaky wave structures.

Dr. Li was awarded the Outstanding Research Thesis Award from City University of Hong Kong in 2015. He received the Best Paper Award at the 2015 IEEE Asia-Pacific Conference on Antennas and Propagation (APCAP), the Best Student Paper at 2013 National Conference on Antennas, and the Best Student Paper Award (2nd Prize) at the 2013 IEEE International Workshop on Electromagnetics (iWEM). He was selected as a Finalist in the student paper contest of 2015 IEEE AP-S Symposium on Antennas and Propagation (APS). He has served as a Reviewer for the IEEE Transactions on Antennas and Propagation, the IEEE Antennas and Wireless Propagation Letters, and the IET Microwaves, Antennas & Propagation.

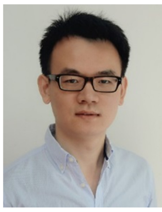

Lei Ge (S'11–M'15) was born in Jiangsu, China. He received the B.S. degree in electronic engineering from Nanjing University of Science and Technology, Nanjing, China, in 2009 and the Ph.D. degree in electronic engineering from City University of Hong Kong, Hong Kong, in 2015. From September 2010 to July 2011, he was a Research Assistant with the City University of Hong Kong. From April 2015 to October 2015, he was a Postdoctoral Research Fellow at the State Key Laboratory of Millimeter Waves, City University of Hong Kong. He is currently Assistant Professor and Associate Head of Department of Electronic Engineering at Shenzhen University, China.

He received the Honorable Mention at the student contest of 2012 IEEE APS-URSI Conference and Exhibition held in Chicago, US. He won the 1st Prize in the Student Innovation Competition of 2014 IEEE International Workshop on Electromagnetics (IEEE iWEM) held in Sapporo, Japan, in 2014. He was the Session Chair of the iWEM 2017 and ACES-China 2017. He was the TPC Member of the APCAP 2016. His recent research interest focuses on wideband antennas, patch antennas, base station antennas, reconfigurable antennas, the antennas for cognitive radio, and filtering antennas.

Junhong Wang (M'02–SM'03) was born in Jiangsu, China, in 1965. He received the B.S. and M.S. degrees in electrical engineering from the University of Electronic Science and Technology of China, Chengdu, China, in 1988 and 1991, respectively, and the Ph.D. degree in electrical engineering from Southwest Jiaotong University, Chengdu, China, in 1994. In 1995, he joined as the Faculty with the Department of Electrical Engineering, Beijing Jiaotong University, Beijing, China, where he became a Professor in 1999. From January 1999 to June 2000, he was a Research Associate with the Department of Electric Engineering, City University of Hong Kong, Kowloon Tong, Hong Kong. From July 2002 to July 2003, he was a Research Scientist with Temasek Laboratories, National University of Singapore, Singapore. He is currently with the Key Laboratory of all Optical Network and Advanced Telecommunication Network, Ministry of Education of China, Beijing Jiaotong Univeristy, Beijing, China, and also with the Institute of Lightwave Technology, Beijing Jiaotong University, Beijing, China. His research interests include numerical methods, antennas, scattering, and leaky wave structures.

Kwai-Man Luk (M'79–SM'94–F'03) was born and educated in Hong Kong. He received the B.Sc.(Eng.) and Ph.D. degrees in electrical engineering from The University of Hong Kong in 1981 and 1985, respectively.

He joined the Department of Electronic Engineering at City University of Hong Kong in 1985 as a Lecturer. Two years later, he moved to the Department of Electronic Engineering at The Chinese University of Hong Kong where he spent four years. Professor Luk returned to the City University of Hong Kong in 1992, and he is currently Chair Professor of Electronic Engineering. His recent research interests include design of patch, planar and dielectric resonator antennas, and microwave measurements. He is the author of 3 books, 9 research book chapters, over 300 journal papers and 220 conference papers. He was awarded 5 US and more than 10 PRC patents on the design of a wideband patch antenna with an L-shaped probe feed. He was Technical Program Chairperson of the 1997 Progress in Electromagnetics Research Symposium (PIERS), General Vice-Chairperson of the 1997 and 2008 Asia-Pacific Microwave Conference (APM including C), General Chairman of the 2006 IEEE Region Ten Conference (TENCON), Technical Program Co-Chairperson of 2008 International Symposium on Antennas and Propagation (ISAP), and General Co-Chairperson of 2011 IEEE International

Workshop on Antenna Technology (IWAT). Professor Luk received the Japan Microwave Prize, at the 1994 Asia Pacific Microwave Conference held in Chiba in December 1994 and the Best Paper Award at the 2008 International Symposium on Antennas and Propagation held in Taipei in October 2008. He was awarded the very competitive 2000 Croucher Foundation Senior Research Fellow in Hong Kong. He received the 2011 State Technological Invention Award (2nd Honor) of China. He was a Chief Guest Editor for a special issue on "Antennas in Wireless Communications" published in the Proceedings of the IEEE in July 2012. He is a Deputy Editor-in-Chief of PIERS journals. Professor Luk is a Fellow of the Chinese Institute of Electronics, PRC, a Fellow of the Institution of Engineering and Technology, UK, a Fellow of the Institute of Electrical and Electronics Engineers, USA and a Fellow of the Electromagnetics Academy, USA.